ACS Infectious Diseases

Article

Cite This: ACS Infect. Dis. 2019, 5, 353−364

pubs.acs.org/journal/aidcbc

Elucidation of a Human Urine Metabolite as a Seryl-Leucine Glycopeptide and as a Biomarker of Effective Anti-Tuberculosis Therapy

Bryna L. Fitzgerald,[†] M. Nurul Islam,[†] Barbara Graham,[†] Sebabrata Mahapatra,[†] Kristofor Webb,[†] W. Henry Boom,[‡,§] Stephanus T. Malherbe,[∥] Moses L. Joloba,[#] John L. Johnson,[‡,§] Jill Winter,[⊥] Gerhard Walzl,[∥] and John T. Belisle*[,†]

[†]Mycobacteria Research Laboratories, Department of Microbiology, Immunology and Pathology, Colorado State University, 200 West Lake Street, 0922 Campus Delivery, Fort Collins, Colorado 80523, United States

[‡]Department of Medicine, Tuberculosis Research Unit (TBRU), Case Western Reserve University, 10900 Euclid Avenue, Cleveland, Ohio 44106, United States

[§]Uganda-Case Western Reserve University Research Collaboration, 28A Upper Kololo Terrace, Kampala, Uganda

[∥]DST/NRF Centre of Excellence for Biomedical Tuberculosis Research and MRC Centre for Molecular and Cellular Biology, Division of Molecular Biology and Human Genetics, Faculty of Medicine and Health Sciences, Stellenbosch University, P.O. Box 241, Francie van Zijl Drive, Cape Town 8000, South Africa

[⊥]Catalysis Foundation for Health, 2100 Addison Street, Berkeley, California 94704, United States

[#]School for Biomedical Sciences, Makerere University, P.O. Box 7062, Kampala, Uganda

Supporting Information

ABSTRACT: The evaluation of new tuberculosis (TB) therapies is limited by the paucity of biomarkers to monitor treatment response. Previous work detected an uncharacterized urine metabolite with a molecular mass of 874.3547 Da that showed promise as a biomarker for successful TB treatment. Using mass spectrometry combined with enzymatic digestions, the metabolite was structurally characterized as a seryl-leucine core 1 *O*-glycosylated peptide (SLC1G) of human origin. Examination of SLC1G in urine revealed a significant abundance increase in individuals with active TB versus their household contacts and healthy controls. Moreover, differential decreases in SLC1G levels were observed by week one in TB patients during successful treatment versus those that failed treatment. The SLC1G levels were also associated with clinical parameters used to measure bacterial burden (GeneXpert) and inflammation (positron emission tomography-computed tomography (PET-CT)). These results demonstrate the importance of metabolite identification and provide strong evidence for applying SLC1G as a biomarker of TB treatment response.

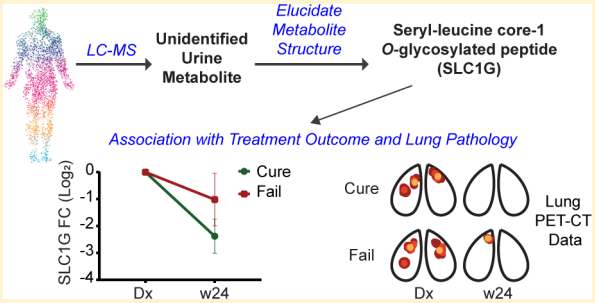

KEYWORDS: *tuberculosis, treatment response, urine metabolite, glycopeptide, core 1 oligosaccharide, mass spectrometry, PET-CT, prognostic biomarker*

Tuberculosis (TB) is the leading cause of mortality worldwide due to an infectious agent, *Mycobacterium tuberculosis* (*Mtb*).[1] A contributing factor to the global burden of TB is the continued emergence of drug resistant *Mtb* strains. Efforts to combat such strains have led to new anti-TB therapies and regimens.[2] Nevertheless, clinical evaluations of new drugs are protracted and typically include a six month treatment regimen with patient follow-up for 12 to 18 months to monitor for disease relapse. These parameters increase the expense of clinical trials and impede the implementation of new drugs for patient care.[2] Thus, identification and validation of biomarkers that provide an early surrogate end point for the long-term outcome of TB treatment has emerged as a research priority.

During the course of *Mtb* infection and treatment, metabolic changes occur in the human host as well as the pathogen.[3] Metabolomics provides a unique tool to capture changes in the profile of small molecule metabolites during infection and treatment. In fact, liquid chromatography−mass spectrometry (LC-MS)-based metabolomics have successfully detected metabolic alterations during the progression from *Mtb* infection to active disease and during anti-TB therapy, supporting the development of metabolite-based biosignatures.[4−6] However, many of the metabolites detected in

Received: September 12, 2018
Published: December 26, 2018

DOI: 10.1021/acsinfecdis.8b00241
ACS Infect. Dis. 2019, 5, 353−364

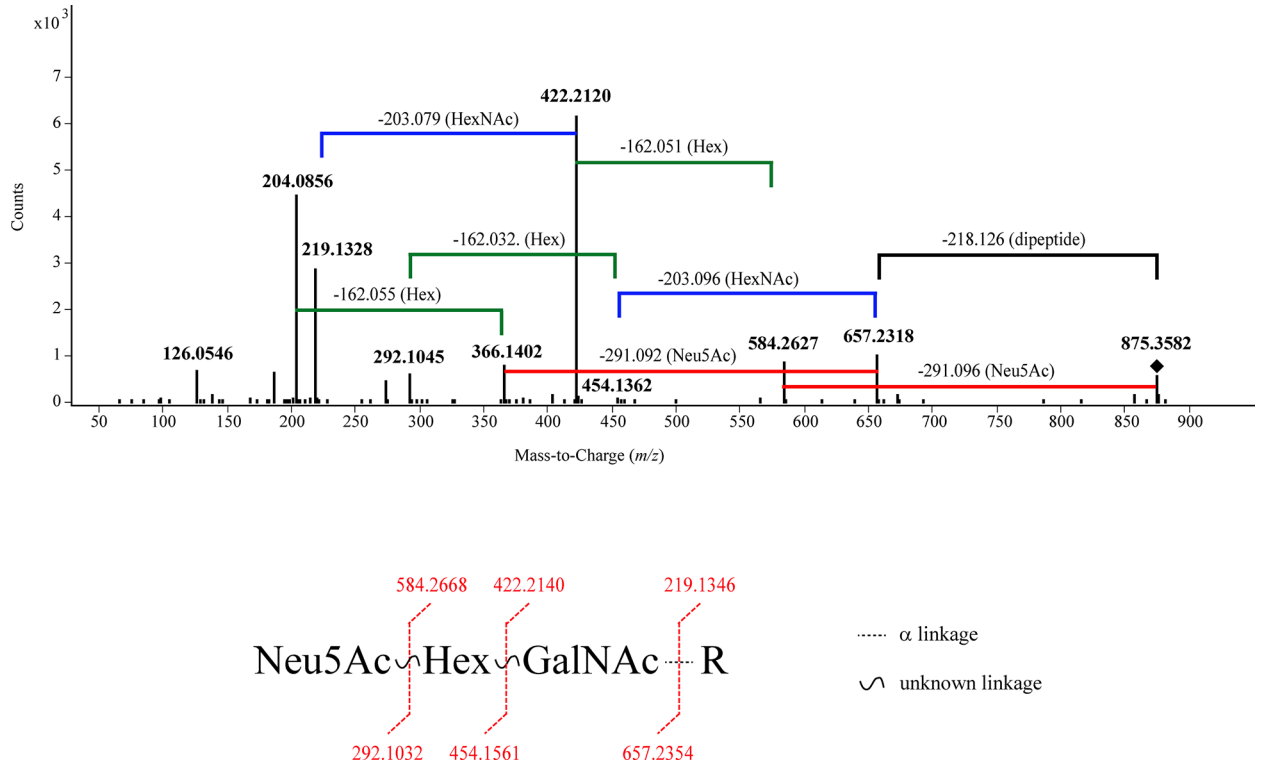

Figure 1. MS/MS interrogation of MF 874.3547 leads to hypothesis of glycopeptide structure. Representative MS/MS spectrum of MF 874.3547 in TB patient urine obtained using collision energy of 20 V (A). Horizontal lines depict neutral losses within the MS/MS spectrum for Neu5Ac (291.09 amu) in red, hexose (162.05 amu) in green, *N*-acetylhexosamine (203.07 amu) in blue, and the unknown dipeptide (218.13 amu) in black. Diagnostic fragment ions for *N*-acetylhexosamine (*m*/*z* 204.0856) and Neu5Ac (*m*/*z* 292.1045) were present. (B) A hypothesized structure with theoretical fragment ions matching those observed in the experimental MS/MS spectrum.

untargeted metabolomics studies remain structurally uncharacterized or only putatively identified and require *de novo* structural identification.[7,8]

Previously, 12 urine metabolites that significantly changed during successful anti-TB treatment were reported. However, five of these metabolites did not match with any compound in available databases, and seven had putative, yet unconfirmed, identifications.[5] The structural characterization of one of these metabolites as *N*-acetylisoputreanine has led to the discovery that alterations in polyamine metabolism occur during TB and response to treatment,[8] an observation now confirmed by others.[9] A second unidentified metabolite designated as molecular feature (MF) 874.3547, on the basis of its monoisotopic mass of 874.3547 Da, decreased in abundance early in the treatment of TB and remained at decreased levels until the end of treatment. In this current study, we applied liquid chromatography (LC) tandem mass spectrometry (MS/MS) combined with enzymatic degradation and analyses of synthetic products to elucidate the structure of MF 874.3547 as a seryl-leucine core 1 *O*-glycosylated peptide (SLC1G). Evaluation of SLC1G in urine from patients with active pulmonary TB (index cases) and their healthy household contacts (HHC) confirmed that this novel urine metabolite is significantly elevated in active TB. Assessment of SLC1G levels in TB patients undergoing standard anti-TB therapy revealed changes in metabolite abundances that are associated with different clinical outcomes (treatment failure, stable long-term cure, or recurrent TB) and measures of inflammation and bacterial load.

RESULTS AND DISCUSSION

MS/MS Analyses of MF 874.3547 Reveal Glycopeptide Fragmentation Patterns. Initial structural information pertaining to MF 874.3547 was obtained by LC-MS/MS fragmentation at different collision energies, with the consistency of the MF 874.3547 fragmentation pattern confirmed using urine samples from six TB patients. MF 874.3547 also was present in commercial and healthy control (HC) urine (Figure S1). A representative MS/MS spectrum of the $[M + H]^+$ adduct (*m*/*z* 875.3582) of MF 874.3547 from one TB patient is shown in Figure 1A. Manual interrogation of the MS/MS spectrum revealed diagnostic fragment ions for *N*-acetylhexosamine (*m*/*z* 204.0856) and *N*-acetylneuraminic acid (Neu5Ac) (*m*/*z* 292.1045), as well as neutral losses corresponding to Neu5Ac (291.09 Da), hexose (162.05 Da), and *N*-acetylhexosamine (203.07 Da) (Figure 1A). Importantly, the fragment ions *m*/*z* 584.2627, *m*/*z* 422.2120, and *m*/*z* 219.1328 represented the sequential loss of Neu5Ac, hexose, and *N*-acetylhexosamine from the parent ion (*m*/*z* 875.3582), respectively. The difference between the parent ion *m*/*z* 875.3582 and the fragment ion *m*/*z* 657.2318 represented a neutral loss of 218.1264 Da that corresponded to the fragment ion *m*/*z* 219.1328 (Figure 1A). These data led to the hypothesis that MF 874.3547 is a glycoconjugate containing an oligosaccharide composed of *N*-acetylhexosamine, hexose, and Neu5Ac (*m*/*z* 657.2318) attached to an unknown structure with a mass of 218.1264 Da (*m*/*z* 219.1328).

Typically, biological glycoconjugates are glycolipids or glycoproteins; thus, the *m*/*z* 219.1328 fragment ion likely represented a lipid or peptide structure. This *m*/*z* value did not

DOI: 10.1021/acsinfecdis.8b00241
ACS Infect. Dis. 2019, 5, 353−364

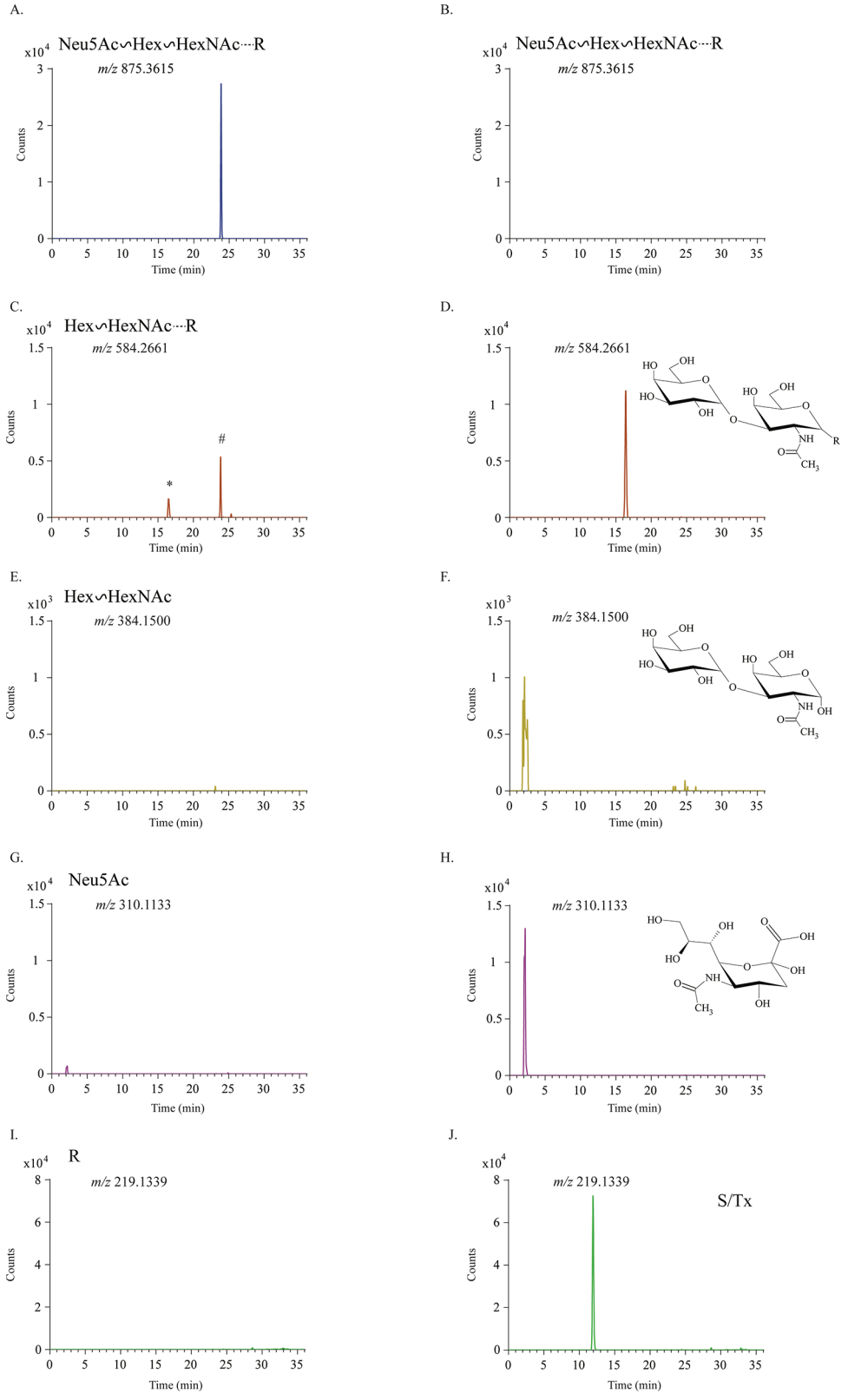

Figure 2. Enzymatic deglycosylation and MS confirmation of core 1 glycosylation. MF 874.3547 untreated (A, C, E, G, I) and treated with α2-3,6,8 neuraminidase and *O*-glycosidase (B, D, F, H, J) were analyzed by LC-MS, and the spectra were evaluated by extracted ion chromatogram (EIC) for intact glycopeptide (A and B), the glycopeptide minus Neu5Ac (C and D), the Hex−HexNAc disaccharide (E and F), Neu5Ac (G and H), and the deglycosylated putative diamino acid S/TX (I and J). The * in panel C indicates a low level of the glycopeptide minus Neu5Ac (m/z 584.2661) present in the undigested sample. Note the level of this product was considerably higher following digestion (G). In source fragmentation of SLC1G yielded the m/z 584.2661 product (# in panel C) at the same retention time as the undigested glycopeptide.

DOI: 10.1021/acsinfecdis.8b00241
ACS Infect. Dis. 2019, 5, 353−364

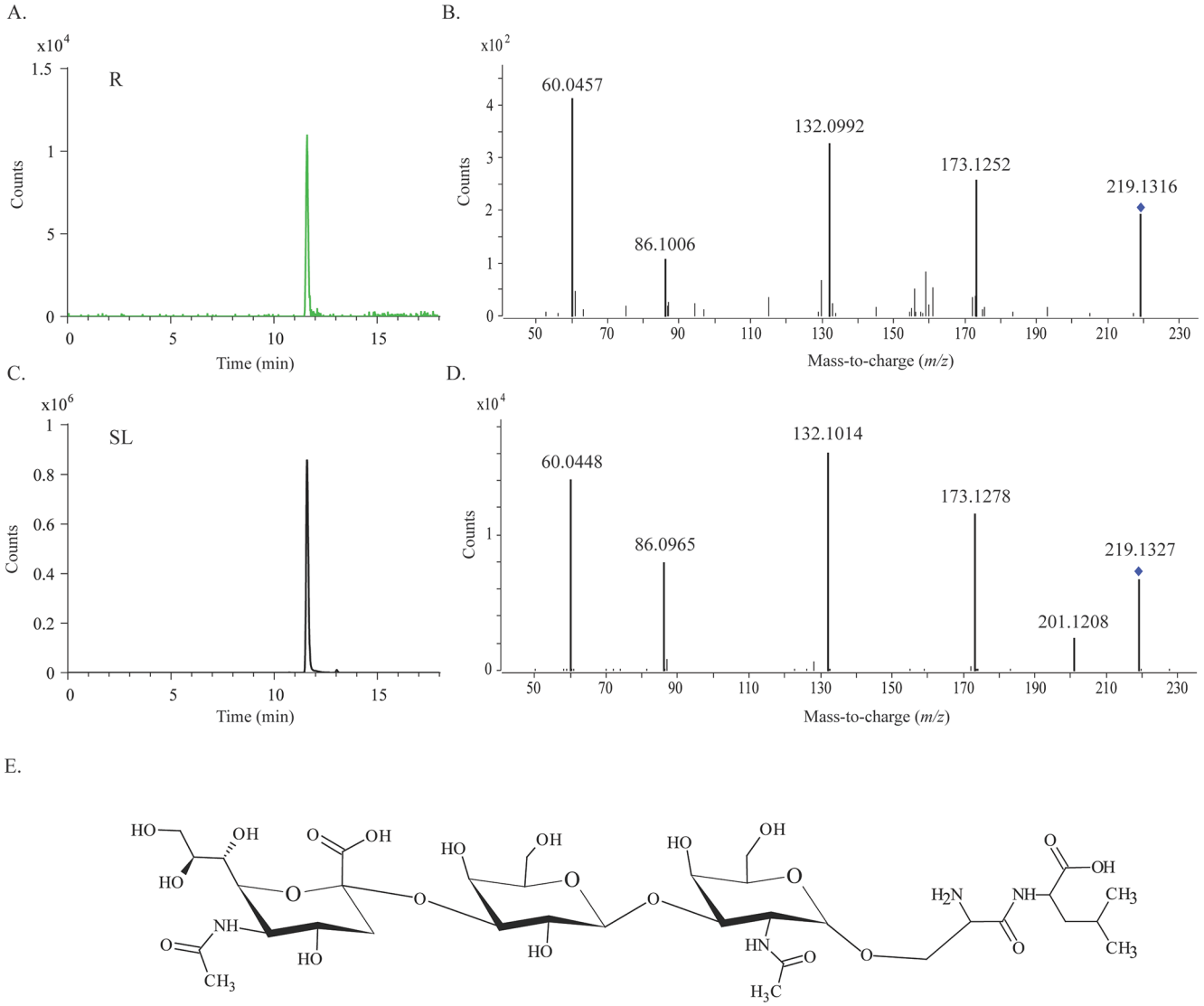

Neu5Acα2-3Galβ1-3GalNAcα1-*O*-SerLeu

Figure 3. Confirmation of seryl-leucine peptide and SLC1G structure. EIC for *m*/*z* 219.1328 in LC-MS spectra of α2-3,6,8 neuraminidase and *O*-glycosidase treated MF 874.3547 (A) and seryl-leucine standard (C). MS/MS of *m*/*z* 219.1328 from α2-3,6,8 neuraminidase and *O*-glycosidase treated MF 874.3547 (B) and the seryl-leucine standard (D). The confirmed structure of Neu5Acα2-3Galβ1-3GalNAcα1-*O*-SerLeu for MF 874.3547 (E).

match any lipid moiety or fragments of glycolipids annotated in existing databases,[10] and the glycosylation pattern of *N*-acetylhexosamine, hexose, and Neu5Ac was similar to that of glycoproteins rather than glycolipids.[11,12] Thus, the *m*/*z* 219.1328 fragment ion was hypothesized to represent a peptide. Glycosylation of glycoproteins typically occurs on asparagine (Asn) residues (*N*-linked), as well as serine (Ser) or threonine (Thr) residues and to a lesser extent tyrosine (Tyr), hydroxylysine, or hydroxyproline residues (*O*-linked).[12−14] Six amino acid combinations that included at least one of these amino acids and possessed a predicted monoisotopic mass of 218.1311 Da were identified: Ser and leucine (Leu) or isoleucine (Ile), or Thr and valine (Val). This indicated an *O*-glycosylated peptide.

The most predominant form of protein *O*-glycosylation is a Ser or Thr residue α linked to *N*-acetylgalactosamine (GalNAc) followed by subsequent sugar moieties and terminating with Neu5Ac.[12,15] Using this information and the fragment ion data (Figure 1A), we developed a hypothesized structure for MF 874.3547 (Figure 1B). *In silico* analysis of this hypothesized structure yielded the fragment ions *m*/*z* 657.2354, 584.2668, 454.1561, 422.2140, 292.1032, and 219.1346 that were observed in the experimental spectrum (Figure 1A).

Confirmation of MF 874.3547 as Seryl-Leucine Core 1 *O*-Glycosylated Peptide (SLC1G). To confirm that the proposed oligosaccharide structure terminated in Neu5Ac, MF 874.3547 was enriched from human urine by HPLC and treated with neuraminidase enzymes.[15] Two neuraminidases, one with specificity for α2-3 terminal Neu5Ac and one with broad specificity for α2-3, α2-6, or α2-8, were applied to MF 874.3547 and commercial standards with α2-3 or α2-6 linked terminal Neu5Ac residues (Figures S2 and S3). LC-MS analyses of the enzymatic digests demonstrated complete

DOI: 10.1021/acsinfecdis.8b00241
ACS Infect. Dis. 2019, 5, 353−364

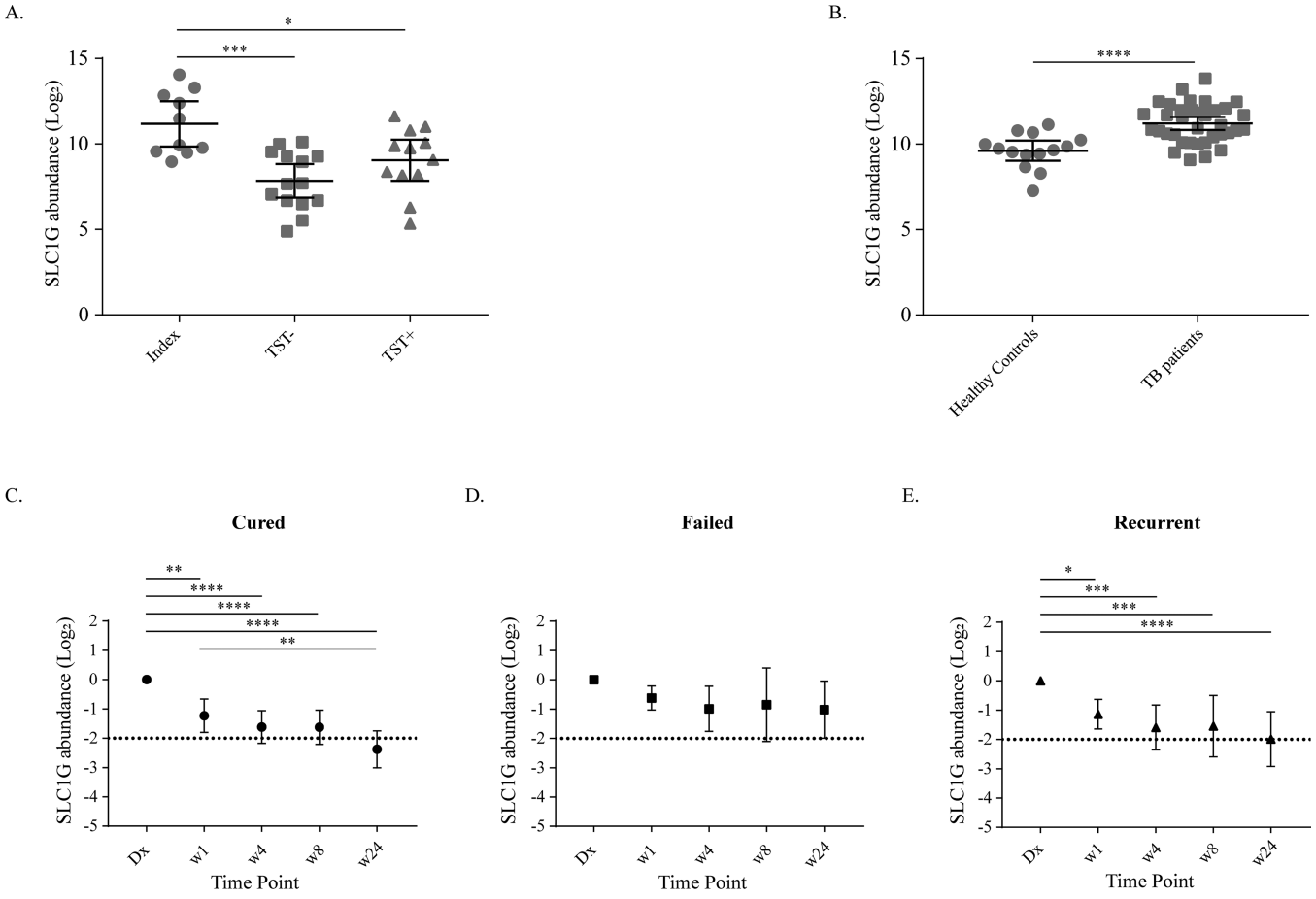

Figure 4. SLC1G levels are associated with active TB and different treatment response outcomes. Log_2 abundances of SLC1G in index TB patients, as compared to TST− and TST+ HHCs of the KCHS (A) and active TB patients at their diagnostic time point and HCs of the Catalysis Study (B). Log_2-fold change in SLC1G levels over 24 weeks of treatment differed in cured (C) and recurrent (E) treatment outcome groups as compared to the failed (D) treatment group. The dashed line indicates a log_2-fold change of −2. Fold changes at each time point are based on SLC1G levels at the Dx time point. The data are representative of index (n = 10), TST− (n = 14), and TST+ (n = 12) patients (A), 14 healthy controls and TB patients (n = 36) (B), and cured (n = 15), failed (n = 8), and recurrent patients (n = 12) (C, D, E). One cured patient was not included in the analysis for (C) due to a missing week 8 time point. Statistical significance was determined using a one-way ANOVA with Tukey's multiple comparison test (A), an unpaired two-tailed t test (B), and a repeated measures one-way ANOVA with Tukey's multiple comparison test (C, D, E). Error bars represent the 95% confidence interval from the mean (*, $p < 0.05$; **, $p < 0.01$; ***, $p < 0.001$; ****, $p < 0.0001$).

hydrolysis of MF 874.3547 with both enzymes. Note the absence of the m/z 875.3582 product and emergence of new products, m/z 310.1130 (Neu5Ac) and m/z 584.2661 (a disaccharide linked dipeptide) in Figure S2. This revealed that the terminal sugar was an α2-3 linked Neu5Ac, as the use of commercial glycopeptide standards demonstrated a linkage other than α2-3 could not be digested with the α2-3 specific neuraminidase. Specifically, the α2-3 neuraminidase digested products with an α2-3 linked Neu5Ac (Figure S3B,C) but not a structure with an α2-6 linked Neu5Ac (Figure S3A).

The disaccharide moiety remaining after digestion with neuraminidase was proposed to be a core 1 oligosaccharide (Galβ1-3GalNAc-), a structure that can be capped with Neu5Ac.[12] To test this, MF 874.3547 was digested with neuraminidase and an *O*-glycosidase possessing endo-α-*N*-acetylgalactosaminidase activity and specificity for core 1 and core 3 *O*-linked disaccharides.[12,15] Treatment of commercial standards with the *O*-glycosidase demonstrated activity consistent with that expected, as this enzyme only digested a commercial standard possessing the core 1 disaccharide (Figure S3C). LC-MS analyses of enriched MF 874.3547 following neuraminidase and *O*-glycosidase treatment resulted in detection of two ions belonging to a disaccharide (m/z 384.1500) and the putative dipeptide (m/z 219.1328), as well as the products observed with the neuraminidase only digest (Figure 2). These data confirmed that MF 874.3547 contained either a core 1 or core 3 *O*-linked disaccharide with a terminal α2-3 linked Neu5Ac. Since core 3 disaccharides are represented by GlcNAcβ1-3GalNAc-, only a core 1 disaccharide was consistent with both the MS/MS spectrum of MF 874.3547 (Figure 1A) and the neuraminidase and *O*-glycosidase treatment data (Figure 2). Thus, the glycosyl structure of MF 874.3547 was confirmed as Neu5Acα2-3Galβ1-3GalNAc.

The structure of the dipeptide was determined by comparing synthetic peptide standards to the retention time and MS/MS spectrum for the m/z 219.1328 product resulting from the neuraminidase and *O*-glycosidase digestion of MF 874.3547. Only the seryl-leucine standard matched both the retention time and MS/MS spectrum of the m/z 219.1328 product (Figures 3 and S4). This confirmed that the entire structure of MF 874.3547 was Neu5Acα2-3Galβ1-3GalNAcα1-*O*-SerLeu, a SLC1G (Figure 3E).

DOI: 10.1021/acsinfecdis.8b00241
ACS Infect. Dis. 2019, 5, 353−364

Naturally occurring peptides are common in the urine of healthy individuals and are mainly products of normal proteolytic degradation that occurs in tissue or body fluids. Altered levels of these peptides may correspond to changes in protein level or protease activity and have been associated with a variety of diseases such as diabetes, chronic kidney disease, and rheumatoid arthritis, as well as aging.[16−19] Although *Mtb* produces *O*-linked glycoproteins, these products possess oligosaccharides of mannose[20] and not the core 1 oligosaccharide structure defined for SLC1G. Additionally, as demonstrated below, SLC1G was identified in urine of healthy controls. Thus, we concluded that SLC1G results from the proteolysis of a host glycoprotein.

The elucidation of MF 874.3547 as SLC1G provides a premise for the structural characterization of additional metabolites identified via untargeted metabolomics experiments and supports the use of host metabolites as indicators of infectious disease. This is not a new concept in TB as host metabolites were being investigated as biomarkers in the 1950s.[21] More recently, Rhee and colleagues[9] revealed several host urine metabolites that distinguished TB patients from those with other pulmonary diseases. These metabolites included sugars contained in the SLC1G structure.

Levels of SLC1G Are Increased in Patients with Active TB Compared to HHC. To establish that increased levels of SLC1G are associated with active TB, the relative abundance of this glycopeptide in active index TB patients and HHCs was evaluated with urine collected under the Kawempe Community Health Study (KCHS).[22] The HHC included both tuberculin skin test (TST) negative (−) and positive (+) individuals. SLC1G levels were significantly higher in the index patients compared to that of HHC (index vs TST−, p = 0.0003; index vs TST+ , p = 0.0255) (Figure 4A). SLC1G was moderately higher in the TST+ group as compared to the TST− group of HHCs, but a significant difference (p = 0.2201) was not obtained (Figure 4A). Using samples from a separate study, the Catalysis Study,[23] a significant difference between urine SLC1G levels in active TB patients at the time of diagnosis and healthy controls was observed (Figure 4B). It is noted that the relative abundance of the SLC1G in the TB patients of the Catalysis Study was similar to that of the SLC1G in the index patients of the KCHS. The increased level of SLC1G in active TB as compared to healthy individuals provides strong evidence that this metabolite is associated with active disease and its initial discovery as a potential treatment response biomarker via untargeted metabolomics[5] was not due to alteration of host metabolism by anti-TB drugs.

Changes in SLC1G Levels Correlate with Different Treatment Response Outcomes. Our previous study that detected SLC1G as a potential biomarker anti-TB treatment did not evaluate whether changes in SLC1G levels during treatment differed between individuals successfully treated versus those that failed treatment.[5] To demonstrate that SLC1G levels could serve as a prognostic biomarker of treatment success, the Catalysis study samples were utilized on the basis of availability of longitudinal patient samples corresponding to different treatment outcomes. We evaluated urine samples from TB patients designated as clinically cured (individuals that converted to sputum culture negative before or at the end of the 24 week treatment and remained culture negative during a two year follow-up) (n = 15), those designated as treatment failures (individuals that remained sputum culture positive at the end of the 24 week treatment) (n = 8), and a group of patients designated as cured but that developed recurrent disease within 18 months of successful treatment (n = 12)[23] (Table 2). The levels of SLC1G at each time point in the cured and failed patient groups were compared using one-way ANOVA with Tukey's multiple comparison test. This demonstrated that the only significant difference in SLC1G levels between these two patient groups was at the week 24 time point (p = 0.038).

However, a comparison of SLC1G levels at baseline (diagnosis) versus treatment time points (1, 4, 8, and 24 weeks) demonstrated a decrease during the first week of treatment in all patient groups; however, the decrease was only significant for the cured and recurrent TB groups (p = 0.0010 and 0.0243, respectively) (Figure 4C−E). Likewise, SLC1G levels at all subsequent time points of treatment (4, 8, and 24 weeks) in comparison to baseline levels differed significantly for the cured and recurrent TB groups but not the treatment failure group (Figure 4). The rapid decrease in urine levels of SLC1G after the start of anti-TB therapy coincides with early periods of treatment when the largest decrease in bacterial load is observed.[24]

The cured patient group also yielded a mean $\log_2$-fold change between baseline and the end of treatment (week 24) that was significantly larger than the fold change at week 1 of treatment (Figures 4 and S5A−C). The magnitude of change in SLC1G levels at weeks 4, 8, and 24 in the failed treatment group was less than in the other groups, with a mean $\log_2$-fold change of around −1. The cured and recurrent TB groups, in comparison, yielded mean $\log_2$-fold changes below −1 (weeks 4 and 8) or below −2 (week 24) (Figures 4 and S5A−C). The lack of a significant decrease in SLC1G levels during the initial intensive phase of therapy (first two months) could have been related to a greatly increased number of missed treatments in this patient group (Table 2). However, the vast majority of missed treatments occurred in the continuation phase, with only one patient having a greater number of missed treatments during the intensive phase.

Overall, SLC1G levels behaved similarly in cured and recurrent TB patients. This observation was not unexpected as the recurrent TB patients were initially designated as cured at the end of treatment (week 24) and developed recurrent TB within one year of successfully completing treatment. Further, it is unknown whether recurrent TB in this patient cohort was due to relapse of treated infections or new infections.[23] The relapse of TB after the completion of anti-TB therapy is an outcome measured during clinical trials and is an important parameter for which biomarkers are needed.[2] Additional studies with longitudinal urine from true relapse patients are required to accurately evaluate the potential value of SLC1G as a biomarker of relapse.

SLC1G Levels Associate with Clinical Measurements of Inflammation and Bacterial Burden. The measurements of bacterial load by GeneXpert MTB/RIF and inflammation by positron emission tomography-computed tomography (PET-CT) imaging are used as indicators of treatment efficacy and disease resolution in clinical studies of anti-TB therapies.[23,25−27] Thus, using the cured and failed treatment groups of the Catalysis Study, we explored whether a relationship existed between SLC1G levels and pulmonary inflammation (PET-CT combined total glycolytic activity (COM TGAI) score) or bacterial load (GeneXpert Ct value) regardless of treatment outcome. Using linear mixed models, a 2-fold increase in SLC1G levels was associated with

DOI: 10.1021/acsinfecdis.8b00241
ACS Infect. Dis. 2019, 5, 353−364

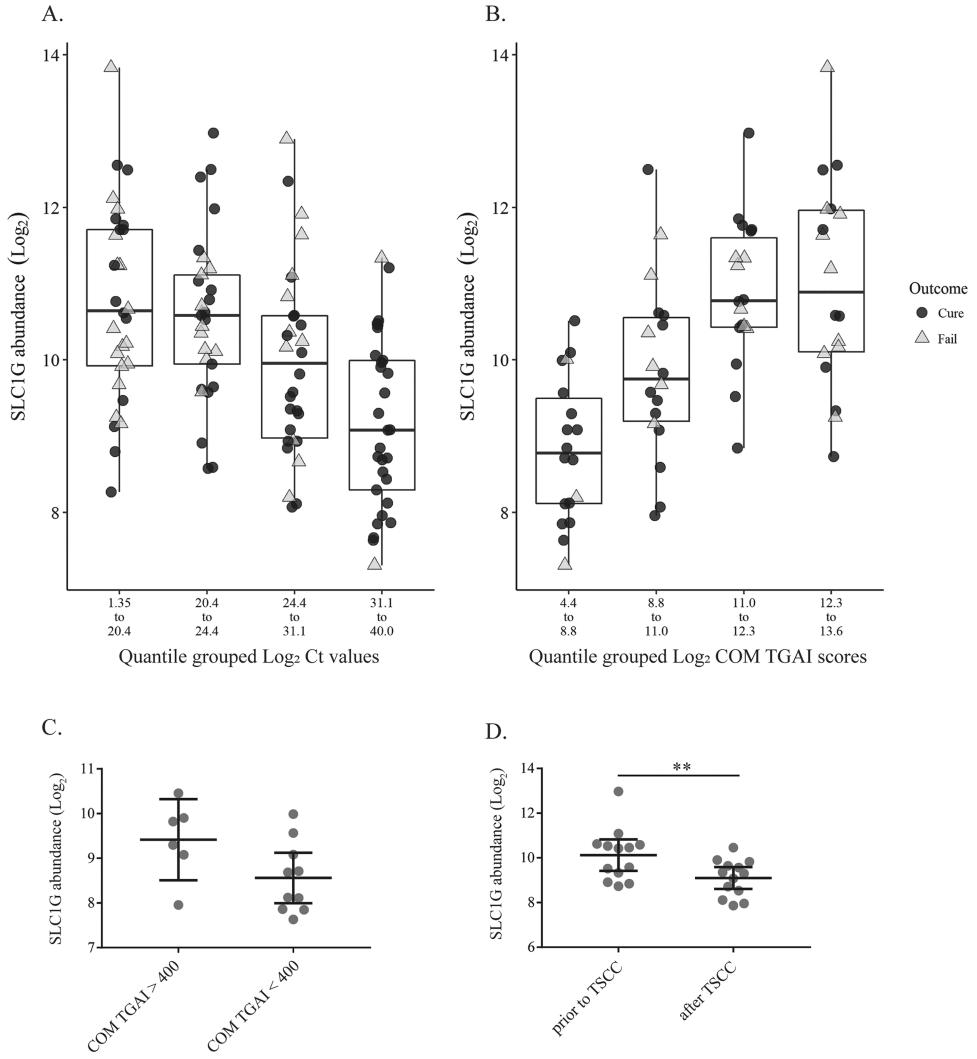

Figure 5. SLC1G levels associate with clinical measurements of bacterial burden and inflammation. Box plot of SLC1G abundances versus quantile grouped GeneXpert MTB/RIF Ct values (A) and COM TGAI scores (B) for all cured and failed patients at all time points. SLC1G abundances trended to increase in cured patients when week 24 COM-TGAI scores indicate persistent inflammation, COM-TGAI scores >400 (C). SLC1G abundances differed significantly in the cured patient population before and after TSCC (D). The data represent patients with COM TGAI > 400 (n = 6) and patients with COM TGAI < 400 (n = 10) (C) and cured patients (n = 13) (D). Three patients were not included in the analysis for (D) due to missing time points before or after sputum culture conversion. Statistical significance was performed with an unpaired two-tailed t test (C) and paired t test (D). Box-and-whiskers plots have lines at the 25th, 50th (median), and 75th percentiles, and the whiskers extend to 1.5 times the interquartile range (A, B). Error bars represent the 95% confidence interval from the mean (C, D) (**, p < 0.01).

an increase in the PET-CT COM TGAI score of 0.82 (95% CI: 0.58−1.06) and a decrease in the GeneXpert MTB/RIF Ct values of 3.2 (95% CI: 2.4−4.5). The COM TGAI provides a single metric to indicate the total burden of lung lesions as measured by PET-CT. To visualize the associations determined using linear mixed models, the COM TGAI scores or GeneXpert MTB/RIF Ct values for all patients and all time points, regardless of treatment outcome, were grouped into four quantiles and plotted against SLC1G $\log_2$ normalized abundances (Figure 5A,B). A positive association occurred between SLC1G levels and increased inflammation (higher COM TGAI scores) (Figure 5A). Likewise, lower SLC1G levels were observed in patients with lower bacterial burdens (i.e., increased GeneXpert MTB/RIF Ct values) (Figure 5B). These associations are also apparent in scatter plots of COM TGAI scores or GeneXpert MTB/RIF Ct values versus SLC1G $\log_2$ normalized abundances for all patients and all time points (Figure S5D,E). The studies of Malherbe et al.[23] revealed that, within the cured patient population, only 16% had resolved their tubercle lesions at the end of treatment. We observed SLC1G levels were increased in the cured patients who remained PET-CT scan positive (i.e., COM-TGAI scores >400) at the end of treatment relative to those that were deemed resolved (Figure 5C). However, this difference was not significant (p = 0.1079).

Time to sputum culture conversion is another end point applied in clinical studies of anti-TB drugs as a measure of bacterial clearance.[28] The SLC1G levels in cured patient samples prior to being designated culture negative were significantly higher (p = 0.0166) than the SLC1G levels in those same patients following conversion to culture negative (Figure 5D). These data establish strong evidence that SLC1G levels were linked with bacterial load and lung pathology in the population study and could be applied to monitor the resolution of disease and infection during treatment.

DOI: 10.1021/acsinfecdis.8b00241
ACS Infect. Dis. 2019, 5, 353−364

Plasma Protease C1 Inhibitor: A Potential Source of SLC1G. To establish a potential origin of SLC1G, the UniProt database was queried for documented glycosylated proteins, resulting in a list of 4508 proteins. Nine proteins with *O*-glycosylation of a Ser-Leu motif were identified. On the basis of previous literature, seven of these proteins were determined to have the glycan structure of SLC1G (Table S1). Whole blood RNaseq data for the Catalysis Study TB patients[29] were interrogated to determine whether any of the levels of the transcripts for these seven proteins followed the same trend as that observed for SLC1G during treatment. The transcript belonging to plasma protease C1 inhibitor (C1INH) decreased approximately 4-fold during treatment, following a similar trend to that of SLC1G (Table S1). One study has reported changes in expression of C1INH transcripts during anti-TB treatment that are similar to the changes we observed in urine levels of SLC1G.[36] Additionally, expression of C1INH transcripts also increases in active TB and household contacts that progress to active disease.[34,35] On the basis of these results, C1INH was highlighted as a plausible precursor protein of the glycosylated dipeptide.

C1INH is an abundant circulating protease inhibitor that regulates complement and coagulation cascades and increases during inflammation.[30] One of the *O*-glycosylation sites in C1INH (Ser-42) possesses an *O*-linked oligosaccharide matching that of SLC1G and is followed by a Leu residue.[31] Other studies have detected C1INH peptides in human urine but not peptides containing the SLC1G motif.[32,33] In addition to C1INH, other proteins possessing the SLC1G glycosylation motif, but that are not annotated as such in the UniProt database, could also be a source of the glycopeptide. Specifically, a glycosylated peptide in the *C*-terminus of fibrinogen alpha chain isoform 2 with the sequence GKPSLSP contains the SLC1G motif. This larger glycopeptide has been identified in urine of individuals with febrile, complicated urinary tract infections.[37] Increased levels of serum fibrinogen and fibrinogen degradation products also are noted to be associated with active TB.[38−40] Although metabolomics measures the cumulative outcome of metabolic processes, changes in the level of small peptides will be influenced by alterations in the production and turnover of transcripts and proteins. This, along with the potential for multiple proteins giving rise to the same peptide, elevates the complexity of studies required to determine the molecular events that influence alterations in the level of specific peptides. Thus, further studies are required to determine whether abundance changes in the SLC1G glycopeptide arise from one or more proteins with this motif or changes in the activity of proteases as has been described to occur during active TB.[41,42]

CONCLUSION

Host metabolic responses provide a means to measure disease severity and patient health. Unfortunately, the implementation of metabolic biomarkers is impeded by a lack of structural identification of potential diagnostic or prognostic metabolites identified via untargeted metabolomics, as well as a scarcity of data associating host metabolites to pathogen load or inflammation. The elucidation of a previously uncharacterized seryl-leucine glycopeptide and measurement of this metabolite in human urine demonstrated that SLC1G levels decreased in association with a reduction of bacterial load and inflammation in patients being treated for TB providing evidence for a specific relationship. The magnitude of change in relative levels of glycopeptide differed between patients that were cured versus those that failed TB treatment, and this difference occurred within the first 2 months of treatment. A limitation of this study was the small number of samples utilized. Thus, future efforts with larger cohorts are necessary to validate SLC1G as a prognostic marker of treatment outcome. It is noted that an absolute quantification of the SLC1G concentration in urine also was not determined. This is part of ongoing efforts to establish quantifiable assays to measure the abundance change in SLC1G and other metabolites during TB treatment. Nevertheless, the data presented provide a basis for development of host metabolite biomarkers to track the early treatment response of TB patients and underscore the value of continuing to structurally elucidate endogenous human metabolites.

METHODS

Study Population. A subset of samples from the DMID 08-0023/TB Trials Consortium NAA2m study conducted in Uganda[5] were used for structural elucidation of MF 874.3547. Patient urine for metabolite quantification was obtained from the TBRU Kawempe Community Health Study (KCHS) conducted in Uganda (http://www.case.edu/affil/tbru/research_dmid01005.html) and the Catalysis Study (Stellenbosch University Human Research Ethics Committee approval number N10/01/013) conducted in Cape Town, South Africa.[23] The KCHS urine samples represented a subset of two cohorts[22] and consisted of 10 index cases of TB and 26 HHC that were TST− (n = 14) and TST+ (n = 12) and were without HIV comorbidity (Table 1). None of the KCHS HHC went on to develop TB. The Catalysis Study urine samples[23] consisted of 14 HC and 35 TB patients with different treatment outcomes: 8 failed treatment, 12 recurrences, and 15 cured (Table 2). All of the available failed and recurrent patients were utilized; however, only a subset of the total cured patient population was utilized to maintain similar sample numbers in each patient group. A posthoc power analysis was performed using the mean SLC1G abundance and standard deviation observed in the HHC samples to ensure adequate power (>80%) for the sample sizes chosen (http://clincalc.com/stats/Power.aspx). All of the parent studies were reviewed and approved by their respective institutional review boards or ethics committees in South Africa, Uganda, and the United States. All participants gave informed consent for study participation and sample retention for future research use.

Table 1. Patient Characteristics, Kawempe Community Household Study (Uganda)

participant characteristics (n = 36)	TB cases (n = 10)	HHC (n = 26)	
		TST− (n = 14)	TST+ (n = 12)
mean age, years (SD)	35 (11)	24 (16)	28 (10)
male, n (%)	1 (10%)	5 (36%)	6 (50%)
location	Uganda	Uganda	Uganda
mean PPD induration, mm (SD)	14 (6)	2 (3)	16 (1)

Urine Processing and Osmolality. Patient urine samples (40 to 45 μL) from the KCHS and Catalysis Study were diluted 1:3 in LC-MS grade water. To produce quality control samples for LC-MS, aliquots (5 μL) of individual urine samples from either KCHS or Catalysis Study were pooled and

DOI: 10.1021/acsinfecdis.8b00241
ACS Infect. Dis. 2019, 5, 353−364

Table 2. Patient Characteristics, Catalysis Study (South Africa)[a]

participant characteristics (n = 48)	TB cases (n = 35)			HC (n = 13)
	cured (n = 15)	recurrence (n = 12)	failure (n = 8)	
mean age, years (SD)	33 (9)	35 (10)	34 (15)	32 (12)
male, n (%)	9 (60%)	7 (58%)	5 (63%)	7 (54%)
previous TB, n (%)	6 (40%)	4 (33%)	4 (50%)	NA
mean treatments missed, n (range of treatments missed)	7 (0−23)	7 (0−32)	43 (0−99)[b]	NA

[a]NA, not applicable. [b]The mean number of missed treatments in the intensive phase (first two months) and continuation phase (two to six months) of treatment were 8 and 35, respectively.

prepared for LC-MS identical to the individual samples. Diluted urine (20 μL) osmolality[46] was measured by freezing point depression using a Micro-Osmometer Model 210 (Advanced Instruments, Norwood, MA). The instrument was calibrated using both 55 and 850 mOsm standards (Advanced Instruments). The accuracy of the instrument was verified with a Clintrol 290 standard (Advanced Instruments).

MF 874.3547 Isolation and Digestion. MF 874.3547 was isolated from human urine (Gemini Bio-Products, West Sacramento, CA) using the LC conditions previously described.[5] Fractions of 0.25 mL were collected from 18 replicate LC runs. Fractions within ±1 min of the target retention time for MF 874.3547 were analyzed by LC-MS for the presence of MF 874.3547. Fractions containing the MF 874.3547 were dried by SpeedVac and stored at −20 °C. The stored fractions were suspended in 70 μL of water before analyses.

MF 874.3547 (9 μL) or standards (60 ng) of 4-nitrophenyl *O*-(*N*-acetyl-α-neuraminosyl)-(2-6)-β-D-galactopyranosyl-(1-4)-2-acetamido-2-deoxy-β-D-glucopyranoside (EN4614, Carbosynth Ltd., San Diego, CA), glycan-F58 (ULM-10078-CA, Cambridge Isotope Laboratories, Inc., Tewksbury, MA), and Sialo Anti-Proliferative Factor (GP131025, Sussex Research Laboratories, Ottawa, ON) were treated with α2-3 neuraminidase S (PO743S), α2-3,6,8 neuraminidase (#P0720S, New England Biolabs Inc., Ipswich, MA, USA), and *O*-glycosidase (#P0733S, New England Biolabs Inc.). Specifically, enzymatic digests were performed with α2-3,6,8 neuraminidase (0.05 units), α2-3 neuraminidase S (0.008 units), or *O*-glycosidase (80 units) in 15 μL (final vol) of 1× GlycoBuffer 2 (#B3704, New England Biolabs Inc.) for 1 h at 37 °C. Reactions were stopped with 70% methanol (final concentration) and incubated at −80 °C for 1 h. Precipitated material was removed by centrifugation (18 000*g*). The methanol extracts were collected, dried by SpeedVac, and resuspended in 20 μL of water prior to LC-MS and LC-MS/MS analyses.

LC-MS and LC-MS/MS Analyses. LC was based on a previously described method using either an Agilent 1200 or 1290 series high-performance LC system (Agilent Technologies, Palo Alto, CA, USA) with an Atlantis T3 reverse-phase C18 3.5 μm column (2.1 × 150 mm; Waters Corp., Milford, MA).[5] Injections (5 μL) of each diluted urine sample, enriched MF 875.3547, or standard were made.

MS analyses of Catalysis Study samples and MS/MS analyses for MF 874.3547 and seryl-leucine structural characterization were performed using an Agilent 6520 quadrupole time-of-flight (Q-TOF) instrument equipped with an electrospray ionization source operated in positive ionization mode. The operating conditions were: gas temperature, 300 °C; drying gas, 8 L/min; nebulizer, 45 lb/in^2; capillary voltage, 2000 V; fragmentation energy, 120 V; skimmer, 60 V; octapole RF setting, 750 V. Specified ions were isolated for MS/MS fragmentation using a mass window of 1.3 Da. Collision induced dissociation was performed with collision energies of 5 to 40 V. Data were collected in the profile and centroid modes at a scan rate of 1.2 spectra/s and a scan range of m/z 100 to 1700 for MS and a scan rate of 2.0 spectra/s and a scan range of m/z 100 to 1700 for MS/MS using the Agilent MassHunter Data Acquisition software.

MS analyses of KCHS samples, enriched MF 874.3547, and Sialo Anti-Proliferative Factor glycopeptide were performed using an Agilent 6230 time-of-flight (TOF) instrument with an electrospray ionization source operated in positive ionization mode. The operating conditions for the mass spectrometer were: gas temperature, 300 °C; drying gas, 11 L/min; nebulizer, 40 lb/in^2; capillary voltage, 2000 V; fragmentation energy, 120 V; skimmer, 60 V; octapole RF setting, 750 V.

MS analyses of Glycan F58 and 4-nitrophenyl *O*-(*N*-acetyl-α-neuraminosyl)-(2-6)-β-D-galactopyranosyl-(1-4)-2-acetamido-2-deoxy-β-D-glucopyranoside were performed using an Agilent 6224 TOF instrument with an electrospray ionization source operated in negative ionization mode. The operating conditions for the mass spectrometer were: gas temperature, 325 °C; drying gas, 7 L/min; nebulizer, 40 lb/in^2; capillary voltage, 3500 V; fragmentation energy, 160 V; skimmer, 60 V; octapole RF setting, 750 V. Data were collected on TOF instruments in the profile and centroid modes at a scan rate of 1.0 spectra/s and a scan range of m/z 100 to 1700.

All patient samples were randomly assigned to batches and analyzed by LC-MS in random order to avoid a patient group bias based on SLC1G stability.

Analyses of MS/MS Spectra and LC-MS Data. The MS/MS spectra were manually interrogated against the METLIN database, the Human Metabolome Database (HMDB), and the NIST/EPA/NIH Mass Spectral Library.[43−45] Theoretical fragment ions of MF 874.3547 were obtained using an ACD/MS Fragmenter (Advanced Chemistry Development, Inc., Toronto, ON).

The LC-MS peak area of MF 874.3547 was used as the SLC1G abundance in individual samples. The LC-MS peak area of MF 874.3547 was normalized to the osmolality of the corresponding sample as this is described as the gold standard for estimating urinary concentration.[46] Normalized abundance values were $\log_2$ transformed and used to interrogate significant differences in SLC1G levels between patient groups using statistical analyses in GraphPad Prism version 6.04 for Windows (GraphPad Software, La Jolla, California, USA). Linear mixed models were performed using R version 3.4.2[47] with the lme4 package and a random subject effect to account for repeated measures.[48] Data used for the linear mixed models were from TB patients of the Catalysis Study and included combined total glycolytic activity (COM TGAI) from PET-CT measurements and GeneXpert MTB/RIF Ct values as the response variable and the normalized $\log_2$ SLC1G abundance value from the same patient as the independent variable. The COM TGAI is an aggregate value consisting of the TGAI and cavity volume and was calculated using the formula COM TGAI = [metabolic lesion volume (PET) × mean metabolic

DOI: 10.1021/acsinfecdis.8b00241
ACS Infect. Dis. 2019, 5, 353−364

lesion intensity (PET)] + [cavity volume (CT) × mean metabolic lesion intensity (PET)]. PET-CT data are available through the Catalysis Biomarker Consortium Data Repository (https://codr.c-path.org/main/home.html).

Data Repositories. Whole blood RNaseq data for the Catalysis Study was obtained from the NCBI GEO database, accession GSE89403. LC-MS data of SLC1G in patient urine and MS/MS data for SLC1G structural elucidation have been deposited in Metabolomics Workbench, Study IDs: ST001104 and ST001069. The SLC1G structure has been deposited in the PubChem database, Pub Chem CID: 134687025.

■ ASSOCIATED CONTENT

Supporting Information

The Supporting Information is available free of charge on the ACS Publications website at DOI: 10.1021/acsinfecdis.8b00241.

Figure S1, presence of SLC1G in TB patients and healthy controls; Figure S2, demonstration of Neu5Ac with an α2-3 linkage as the terminal sugar of SLC1G; Figure S3, activity of α2-3 neuraminidase or α2-3,6,8 neuraminidase and *O*-glycosidase on commercial oligosaccharide standards; Figure S4, LC-MS chromatograms of diamino acid standards and of α2-3,6,8 neuraminidase and *O*-glycosidase treated SLC1G; Figure S5, fold change of SLC1G levels during treatment and SLC1G abundance associations to GeneXpert and PET-CT measurements based on individual patients; Table S1, transcript levels for potential SLC1G source protein in Catalysis Study patients (PDF)

■ AUTHOR INFORMATION

Corresponding Author

*E-mail: john.belisle@coloradostate.edu. Phone: 970 491-5384.

ORCID

John T. Belisle: 0000-0002-2539-2798

Author Contributions

B.L.F., M.N.I., S.M., K.W., and J.T.B. designed the experiments for structural identification of SLC1G and analyzed and interpreted MS/MS data. B.L.F., J.T.B., J.W., G.W., and W.H.B. designed the experiments for evaluation of SLC1G as a biomarker in human urine. B.L.F., J.T.B., J.W., G.W., W.H.B., and S.T.M. interpreted data correlating SLC1G levels with clinical outcomes and measurements. G.W., W.H.B, J.L.J., and M.L.J. provided clinical samples and clinical data. B.L.F. performed the experiments. B.G. performed statistical analyses. B.L.F. and J.T.B. wrote the manuscript with contributions from all other authors. All authors provided critical feedback and helped shape the research, analysis, and manuscript.

Notes

The authors declare no competing financial interest.

■ ACKNOWLEDGMENTS

The work was supported by the U.S. NIH (U01 AI-115619 to J.T.B. and G.W. and HHSN266200700022C/NO1-AI-70022 to W.H.B.) and the Bill and Melinda Gates Foundation (OPP1039669 to J.T.B. and OPP51919 to G.W.). We thank Dr. Patrick McCue and Paula Moffett (Colorado State University) for allowing use of their Micro-Osmometer Model 210.

■ ABBREVIATIONS

Mtb, *Mycobacterium tuberculosis*; SLC1G, seryl-leucine core 1 *O*-glycosylated peptide; LC-MS, liquid chromatography−mass spectrometry; HHC, household contacts; HC, healthy controls; Neu5Ac, *N*-acetylneuraminic acid; Gal, galactose; GalNAc, *N*-acetylgalactosamine; KCHS, Kawempe Community Health Study; TST, tuberculin skin test; COM TGAI, PET-CT combined total glycolytic activity; C1INH, plasma protease C1 inhibitor; Q-TOF, quadrupole-time-of-flight; HMDB, Human Metabolome Database

■ REFERENCES

(1) WHO. (2017) *Global Tuberculosis Report*, WHO, Geneva.

(2) Tiberi, S., du Plessis, N., Walzl, G., Vjecha, M. J., Rao, M., Ntoumi, F., Mfinanga, S., Kapata, N., Mwaba, P., McHugh, T. D., Ippolito, G., Migliori, G. B., Maeurer, M. J., and Zumla, A. (2018) Tuberculosis: progress and advances in development of new drugs, treatment regimens, and host-directed therapies. *Lancet Infect. Dis. 18*, e183−e198.

(3) Olive, A. J., and Sassetti, C. M. (2016) Metabolic crosstalk between host and pathogen: sensing, adapting and competing. *Nat. Rev. Microbiol. 14*, 221−234.

(4) Das, M. K., Bishwal, S. C., Das, A., Dabral, D., Badireddy, V. K., Pandit, B., Varghese, G. M., and Nanda, R. K. (2015) Deregulated tyrosine-phenylalanine metabolism in pulmonary tuberculosis patients. *J. Proteome Res. 14*, 1947−1956.

(5) Mahapatra, S., Hess, A. M., Johnson, J. L., Eisenach, K. D., DeGroote, M. A., Gitta, P., Joloba, M. L., Kaplan, G., Walzl, G., Boom, W. H., and Belisle, J. T. (2014) A metabolic biosignature of early response to anti-tuberculosis treatment. *BMC Infect. Dis. 14*, 53.

(6) Weiner, J., Parida, S. K., Maertzdorf, J., Black, G. F., Repsilber, D., Telaar, A., Mohney, R. P., Arndt-Sullivan, C., Ganoza, C. A., Faé, K. C., Walzl, G., and Kaufmann, S. H. (2012) Biomarkers of inflammation, immunosuppression and stress with active disease are revealed by metabolomic profiling of tuberculosis patients. *PLoS One 7*, No. e40221.

(7) Dunn, W. B., Erban, A., Weber, R. J. M., Creek, D. J., Brown, M., Breitling, R., Hankemeier, T., Goodacre, R., Neumann, S., Kopka, J., and Viant, M. R. (2013) Mass appeal: metabolite identification in mass spectrometry-focused untargeted metabolomics. *Metabolomics 9*, 44−66.

(8) Fitzgerald, B. L., Mahapatra, S., Farmer, D. K., McNeil, M. R., Casero, R. A., and Belisle, J. T. (2017) Elucidating the structure of *N*-1-Acetylisoputreanine: A novel polyamine catabolite in human urine. *ACS Omega 2*, 3921−3930.

(9) Isa, F., Collins, S., Lee, M. H., Decome, D., Dorvil, N., Joseph, P., Smith, L., Salerno, S., Wells, M. T., Fischer, S., Bean, J. M., Pape, J. W., Johnson, W. D., Fitzgerald, D. W., and Rhee, K. Y. (2018) Mass spectrometric identification of urinary biomarkers of pulmonary tuberculosis. *EBioMedicine 31*, 157−165.

(10) Sud, M., Fahy, E., Cotter, D., Brown, A., Dennis, E. A., Glass, C. K., Merrill, A. H., Murphy, R. C., Raetz, C. R. H., Russell, D. W., and Subramaniam, S. (2007) LMSD: LIPID MAPS structure database. *Nucleic Acids Res. 35*, D527−D532.

(11) Maccioni, H. J. F., Quiroga, R., and Spessott, W. (2011) Organization of the synthesis of glycolipid oligosaccharides in the golgi complex. *FEBS Lett. 585*, 1691−1698.

(12) Varki, A. (1999) *Essentials of glycobiology*, second ed., Cold Spring Harbor Laboratory Press, Cold Spring Harbor, NY.

(13) Halim, A., Brinkmalm, G., Ruetschi, U., Westman-Brinkmalm, A., Portelius, E., Zetterberg, H., Blennow, K., Larson, G., and Nilsson, J. (2011) Site-specific characterization of threonine, serine, and tyrosine glycosylations of amyloid precursor protein/amyloid beta-peptides in human cerebrospinal fluid. *Proc. Natl. Acad. Sci. U. S. A. 108*, 11848−11853.

(14) Song, E. W., and Mechref, Y. (2013) LC-MS/MS identification of the *O*-glycosylation and hydroxylation of amino acid residues of

DOI: 10.1021/acsinfecdis.8b00241
ACS Infect. Dis. 2019, 5, 353−364

collagen alpha-1 (II) chain from bovine cartilage. *J. Proteome Res. 12*, 3599−3609.
(15) Kobata, A. (1979) Use of endo- and exoglycosidases for structural studies of glycoconjugates. *Anal. Biochem. 100*, 1−14.
(16) Good, D. M., Zürbig, P., Argilés, A., Bauer, H. W., Behrens, G., Coon, J. J., Dakna, M., Decramer, S., Delles, C., Dominiczak, A. F., Ehrich, J. H., Eitner, F., Fliser, D., Frommberger, M., Ganser, A., Girolami, M. A., Golovko, I., Gwinner, W., Haubitz, M., Herget-Rosenthal, S., Jankowski, J., Jahn, H., Jerums, G., Julian, B. A., Kellmann, M., Kliem, V., Kolch, W., Krolewski, A. S., Luppi, M., Massy, Z., Melter, M., Neusüss, C., Novak, J., Peter, K., Rossing, K., Rupprecht, H., Schanstra, J. P., Schiffer, E., Stolzenburg, J. U., Tarnow, L., Theodorescu, D., Thongboonkerd, V., Vanholder, R., Weissinger, E. M., Mischak, H., and Schmitt-Kopplin, P. (2010) Naturally occurring human urinary peptides for use in diagnosis of chronic kidney disease. *Mol. Cell. Proteomics 9*, 2424−2437.
(17) Nkuipou-Kenfack, E., Bhat, A., Klein, J., Jankowski, V., Mullen, W., Vlahou, A., Dakna, M., Koeck, T., Schanstra, J. P., Zürbig, P., Rudolph, K. L., Schumacher, B., Pich, A., and Mischak, H. (2015) Identification of ageing-associated naturally occurring peptides in human urine. *Oncotarget 6*, 34106−34117.
(18) Stalmach, A., Johnsson, H., McInnes, I. B., Husi, H., Klein, J., Dakna, M., Mullen, W., Mischak, H., and Porter, D. (2014) Identification of urinary peptide biomarkers associated with rheumatoid arthritis. *PLoS One 9*, No. e104625.
(19) Zhang, M., Fu, G., and Lei, T. (2015) Two urinary peptides associated closely with type 2 diabetes mellitus. *PLoS One 10*, No. e0122950.
(20) Dobos, K. M., Khoo, K. H., Swiderek, K. M., Brennan, P. J., and Belisle, J. T. (1996) Definition of the full extent of glycosylation of the 45-kilodalton glycoprotein of *Mycobacterium tuberculosis*. *J. Bacteriol. 178*, 2498−2506.
(21) Makino, K., Satoh, K., Fujiki, T., and Kawaguchi, K. (1952) Relation of 3-hydroxykynurenine to the ehrlich diazo reaction of urine in severe tuberculosis. *Nature 170*, 977−978.
(22) Guwatudde, D., Nakakeeto, M., Jones-Lopez, E. C., Maganda, A., Chiunda, A., Mugerwa, R. D., Ellner, J. J., Bukenya, G., and Whalen, C. C. (2003) Tuberculosis in household contacts of infectious cases in Kampala, Uganda. *Am. J. Epidemiol. 158*, 887−898.
(23) Malherbe, S. T., Shenai, S., Ronacher, K., Loxton, A. G., Dolganov, G., Kriel, M., Van, T., Chen, R. Y., Warwick, J., Via, L. E., Song, T., Lee, M., Schoolnik, G., Tromp, G., Alland, D., Barry, C. E., Winter, J., Walzl, G., et al. (2016) Persisting positron emission tomography lesion activity and *Mycobacterium tuberculosis* mRNA after tuberculosis cure. *Nat. Med. 22*, 1094−1100.
(24) Donald, P. R., and Diacon, A. H. (2008) The early bactericidal activity of anti-tuberculosis drugs: a literature review. *Tuberculosis 88*, S75−S83.
(25) Blakemore, R., Story, E., Helb, D., Kop, J., Banada, P., Owens, M. R., Chakravorty, S., Jones, M., and Alland, D. (2010) Evaluation of the analytical performance of the Xpert MTB/RIF assay. *J. Clin. Microbiol. 48*, 2495−2501.
(26) Shenai, S., Ronacher, K., Malherbe, S., Stanley, K., Kriel, M., Winter, J., Peppard, T., Barry, C. E., Wang, J., Dodd, L. E., Via, L. E., Walzl, G., Alland, D., et al. (2016) Bacterial loads measured by the Xpert MTB/RIF assay as markers of culture conversion and bacteriological cure in pulmonary TB. *PLoS One 11*, e0160062.
(27) White, A. G., Maiello, P., Coleman, M. T., Tomko, J. A., Frye, L. J., Scanga, C. A., Lin, P. L., and Flynn, J. L. (2017) Analysis of (18)FDG PET/CT imaging as a tool for studying *Mycobacterium tuberculosis* infection and treatment in non-human primates. *J. Visualized Exp.*, No. e56375.
(28) Holtz, T. H., Sternberg, M., Kammerer, S., Laserson, K. F., Riekstina, V., Zarovska, E., Skripconoka, V., Wells, C. D., and Leimane, V. (2006) Time to sputum culture conversion in multidrug-resistant tuberculosis: Predictors and relationship to treatment outcome. *Ann. Intern. Med. 144*, 650−659.
(29) Thompson, E. G., Du, Y., Malherbe, S. T., Shankar, S., Braun, J., Valvo, J., Ronacher, K., Tromp, G., Tabb, D. L., Alland, D., Shenai, S., Via, L. E., Warwick, J., Aderem, A., Scriba, T. J., Winter, J., Walzl, G., Zak, D. E., Catalysis, T. B. B. C., et al. (2017) Host blood RNA signatures predict the outcome of tuberculosis treatment. *Tuberculosis 107*, 48−58.
(30) Davis, A. E., Mejia, P., and Lu, F. X. (2008) Biological activities of C1 inhibitor. *Mol. Immunol. 45*, 4057−4063.
(31) Bock, S. C., Skriver, K., Nielsen, E., Thogersen, H. C., Wiman, B., Donaldson, V. H., Eddy, R. L., Marrinan, J., Radziejewska, E., Huber, R., Shows, T. B., and Magnusson, S. (1986) Human C1 inhibitor - Primary structure, cDNA cloning, and chromosomal localization. *Biochemistry 25*, 4292−4301.
(32) von Zur Mühlen, C., Koeck, T., Schiffer, E., Sackmann, C., Zürbig, P., Hilgendorf, I., Reinöhl, J., Rivera, J., Zirlik, A., Hehrlein, C., Mischak, H., Bode, C., and Peter, K. (2016) Urine proteome analysis as a discovery tool in patients with deep vein thrombosis and pulmonary embolism. *Proteomics: Clin. Appl. 10*, 574−584.
(33) Wang, Y., Chen, J., Chen, L., Zheng, P., Xu, H. B., Lu, J., Zhong, J., Lei, Y., Zhou, C., Ma, Q., Li, Y., and Xie, P. (2014) Urinary peptidomics identifies potential biomarkers for major depressive disorder. *Psychiatry Res. 217*, 25−33.
(34) Zak, D. E., Penn-Nicholson, A., Scriba, T. J., Thompson, E., Suliman, S., Amon, L. M., Mahomed, H., Erasmus, M., Whatney, W., Hussey, G. D., Abrahams, D., Kafaar, F., Hawkridge, T., Verver, S., Hughes, E. J., Ota, M., Sutherland, J., Howe, R., Dockrell, H. M., Boom, W. H., Thiel, B., Ottenhoff, T. H., Mayanja-Kizza, H., Crampin, A. C., Downing, K., Hatherill, M., Valvo, J., Shankar, S., Parida, S. K., Kaufmann, S. H., Walzl, G., Aderem, A., Hanekom, W. A., and ACS and GC6-74 cohort study groups (2016) A blood RNA signature for tuberculosis disease risk: a prospective cohort study. *Lancet 387*, 2312−2322.
(35) Mehra, S., Alvarez, X., Didier, P. J., Doyle, L. A., Blanchard, J. L., Lackner, A. A., and Kaushal, D. (2013) Granuloma correlates of protection against tuberculosis and mechanisms of immune modulation by *Mycobacterium tuberculosis*. *J. Infect. Dis. 207*, 1115−1127.
(36) Cliff, J. M., Lee, J. S., Constantinou, N., Cho, J. E., Clark, T. G., Ronacher, K., King, E. C., Lukey, P. T., Duncan, K., Van Helden, P. D., Walzl, G., and Dockrell, H. M. (2013) Distinct phases of blood gene expression pattern through tuberculosis treatment reflect modulation of the humoral immune response. *J. Infect. Dis. 207*, 18−29.
(37) Pacchiarotta, T., Hensbergen, P. J., Wuhrer, M., van Nieuwkoop, C., Nevedomskaya, E., Derks, R. J., Schoenmaker, B., Koeleman, C. A., van Dissel, J., Deelder, A. M., and Mayboroda, O. A. (2012) Fibrinogen alpha chain *O*-glycopeptides as possible markers of urinary tract infection. *J. Proteomics 75*, 1067−1073.
(38) Kager, L. M., Blok, D. C., Lede, I. O., Rahman, W., Afroz, R., Bresser, P., van der Zee, J. S., Ghose, A., Visser, C. E., de Jong, M. D., Tanck, M. W., Zahed, A. S., Alam, K. M., Hassan, M., Hossain, A., Lutter, R., Veer, C. V., Dondorp, A. M., Meijers, J. C., and van der Poll, T. (2015) Pulmonary tuberculosis induces a systemic hypercoagulable state. *J. Infect. 70*, 324−334.
(39) Liu, J., Jiang, T., Wei, L., Yang, X., Wang, C., Zhang, X., Xu, D., Chen, Z., Yang, F., and Li, J. C. (2013) The discovery and identification of a candidate proteomic biomarker of active tuberculosis. *BMC Infect. Dis. 13*, 506.
(40) Robson, S. C., White, N. W., Aronson, I., Woollgar, R., Goodman, H., and Jacobs, P. (1996) Acute-phase response and the hypercoagulable state in pulmonary tuberculosis. *Br. J. Haematol. 93*, 943−949.
(41) Reece, S. T., Loddenkemper, C., Askew, D. J., Zedler, U., Schommer-Leitner, S., Stein, M., Mir, F. A., Dorhoi, A., Mollenkopf, H. J., Silverman, G. A., and Kaufmann, S. H. E. (2010) Serine protease activity contributes to control of *Mycobacterium tuberculosis* in hypoxic lung granulomas in mice. *J. Clin. Invest. 120*, 3365−3376.
(42) Al Shammari, B., Shiomi, T., Tezera, L., Bielecka, M. K., Workman, V., Sathyamoorthy, T., Mauri, F., Jayasinghe, S. N., Robertson, B. D., D'Armiento, J., Friedland, J. S., and Elkington, P. T.

DOI: 10.1021/acsinfecdis.8b00241
ACS Infect. Dis. 2019, 5, 353−364

(2015) The extracellular matrix regulates granuloma necrosis in tuberculosis. *J. Infect. Dis. 212*, 463−473.
(43) Smith, C. A., O'Maille, G., Want, E. J., Qin, C., Trauger, S. A., Brandon, T. R., Custodio, D. E., Abagyan, R., and Siuzdak, G. (2005) METLIN: a metabolite mass spectral database. *Ther. Drug Monit. 27*, 747−751.
(44) Wishart, D. S., Jewison, T., Guo, A. C., Wilson, M., Knox, C., Liu, Y., Djoumbou, Y., Mandal, R., Aziat, F., Dong, E., Bouatra, S., Sinelnikov, I., Arndt, D., Xia, J., Liu, P., Yallou, F., Bjorndahl, T., Perez-Pineiro, R., Eisner, R., Allen, F., Neveu, V., Greiner, R., and Scalbert, A. (2012) HMDB 3.0–The human metabolome database in 2013. *Nucleic Acids Res. 41*, D801−807.
(45) Simón-Manso, Y., Lowenthal, M. S., Kilpatrick, L. E., Sampson, M. L., Telu, K. H., Rudnick, P. A., Mallard, W. G., Bearden, D. W., Schock, T. B., Tchekhovskoi, D. V., Blonder, N., Yan, X., Liang, Y., Zheng, Y., Wallace, W. E., Neta, P., Phinney, K. W., Remaley, A. T., and Stein, S. E. (2013) Metabolite profiling of a NIST Standard Reference Material for human plasma (SRM 1950): GC-MS, LC-MS, NMR, and clinical laboratory analyses, libraries, and web-based resources. *Anal. Chem. 85*, 11725−11731.
(46) Chadha, V., Garg, U., and Alon, U. S. (2001) Measurement of urinary concentration: a critical appraisal of methodologies. *Pediatr. Nephrol. 16*, 374−382.
(47) R Core Team. (2017) *R: A language and environment for statistical computing*, R Foundation for Statistical Computing, Vienna, Austria.
(48) Bates, D., Machler, M., Bolker, B. M., and Walker, S. C. (2015) Fitting linear mixed-effects models using lme4. *J. Stat. Software 67*, 1−48.

DOI: 10.1021/acsinfecdis.8b00241
ACS Infect. Dis. 2019, 5, 353−364